Teaching old indices new tricks: A state-space analysis of El Niño related climate indices

Roy Mendelssohn, Steven J. Bograd, Franklin B. Schwing, and Daniel M. Palacios
Pacific Fisheries Environmental Laboratory, Southwest Fisheries Science Center, Pacific Grove, California, USA

Received 3 January 2005; revised 3 March 2005; accepted 22 March 2005; published 12 April 2005.

[1] State-space models were applied to several climate indices associated with the El Niño–Southern Oscillation (ENSO), including the Southern Oscillation Index (SOI) and its component sea level pressure series; the NINO3 sea surface temperature index; and the Northern Oscillation Index (NOI). The best models for each series include a significant long-term nonparametric trend combined with a stochastic stationary cyclic term that clearly delineates the El Niño and La Niña events. There is no evidence that the frequency of ENSO events has changed over the 20th century. The long-term trend, however, has contributed to an apparent increase in the magnitude of recent El Niño events. This trend, potentially related to global warming, has increased the level of each series by an amount equal to 30–50% of the amplitude of their corresponding annual cycle or cyclic ENSO term. Thus, the background sea surface temperature in the eastern equatorial Pacific is more than 0.5°C warmer now than prior to 1950, implying a greater overall impact of El Niño events. **Citation:** Mendelssohn, R., S. J. Bograd, F. B. Schwing, and D. M. Palacios (2005), Teaching old indices new tricks: A state-space analysis of El Niño related climate indices, *Geophys. Res. Lett.*, *32*, L07709, doi:10.1029/2005GL022350.

1. Introduction

[2] Among the most commonly used and analyzed sets of climate time series are the El Niño indices such as the Southern Oscillation Index (SOI) [*Horel and Wallace*, 1981; *Philander*, 1990; *Trenberth*, 1984; *Trenberth and Hoar*, 1996; *Trenberth and Shea*, 1987] and the related NINO.x sea surface temperature indices [*Mann et al.*, 2000; *Trenberth*, 1997]. Given their frequent use in the literature, it would seem unlikely that much new information could be extracted from further analysis of these indices. We present a state-space decomposition and analysis of the SOI, its component sea level pressure (SLP) series (Darwin and Tahiti), and the NINO3 index, that shows that each index contains a significant, yet previously unidentified, underlying trend separate from the El Niño-Southern Oscillation (ENSO) signal. The ENSO signal is best reflected in a stochastic but stationary cycle, and the SOI index no better reflects the El Niño events than do the individual pressure series that comprise it. These results imply that the ENSO cycle, though stationary, is superimposed on a long-term trend that is changing the apparent magnitude of the El Niño and La Niña events.

2. Data and Methods

[3] We analyzed the monthly reconstructed SOI from the COADS data set (available from http://tao.atmos.washington.edu/data/soicoads2/), the reconstructed SLP series for Darwin and Tahiti (available from the same site), and a yearly version of the NINO3 index from *Mann et al.* [2000]. This version of the NINO3, which has only a constant mean removed from the series, is used to minimize the effects of other filters or analyses on the data. We also included the Northern Oscillation Index (NOI) [*Schwing et al.*, 2002] (available at http://www.pfeg.noaa.gov) in the analysis in order to examine extratropical effects.

[4] The time series were analyzed using a state-space decomposition [*Harvey*, 1989; *Durbin and Koopman*, 2001], which we have applied previously to examine long-term changes in the mean and seasonal components in many other climate time series [*Mendelssohn et al.*, 2003, 2004, and references therein]. State-space models allow for a series to be decomposed into a variety of different independent components, such as a nonparametric or fixed mean (trend), autoregressive (AR) component, stochastic cycle, stochastic seasonal, etc. As state-space models are statistical models with a well-defined likelihood, model comparison and selection can be performed using criteria such as the AIC [*Akaike*, 1973].

[5] For each series analyzed, we estimated the following models:

[6] 1. A nonparametric trend, a stochastic seasonal (if monthly data), and an observational error term.

[7] 2. Model 1 plus an AR term of order 1.

[8] 3. Model 1 plus one or more stationary stochastic cycles.

[9] 4. All of the above with a fixed mean and/or a deterministic seasonal.

[10] The state-space specification of a stochastic cycle [*Durbin and Koopman*, 2001] is:

$$\begin{bmatrix} \psi_t \\ \psi_t^* \end{bmatrix} = \rho \begin{bmatrix} \cos\lambda_c & \sin\lambda_c \\ -\sin\lambda_c & \cos\lambda_c \end{bmatrix} \begin{bmatrix} \psi_{t-1} \\ \psi_{t-1}^* \end{bmatrix} + \begin{bmatrix} \kappa_t \\ \kappa_t^* \end{bmatrix}, \qquad t = 1, \ldots, T, \tag{1}$$

where ψ_t and ψ_t^* are the states, λ_c is the frequency, in radians, in the range $0 < \lambda_c \leq \pi$, κ_t and κ_t^* are two mutually uncorrelated white noise disturbances with zero means and common variance σ_κ^2, and ρ is a damping factor. The damping factor ρ in (1) accounts for the time over which a higher amplitude event (consider this to be a "shock" to the series) in the stochastic cycle will contribute in subsequent cycles. A stochastic cycle has changing amplitude and phase, and becomes a first order autoregression if λ_c is 0

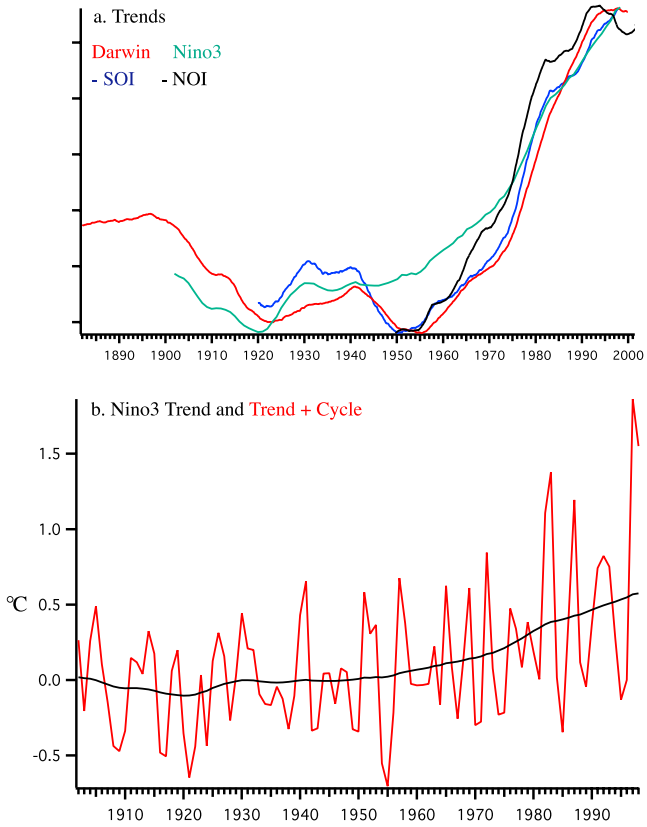

Figure 1. (a) The estimated trend terms for the negative COADS-based SOI (blue, [−0.58, 0.019]), Darwin SLP (red, [97.8, 101.25]), yearly NINO3 (green, [−0.104, 0.575]), and the negative NOI (black, [−0.53, 0.53]). The numbers in brackets give the range of each of the variables on the y-axis. (b) The estimated NINO3 trend (black) and trend plus stochastic cycle (red).

or π. Moreover, it can be shown that as $\rho \rightarrow 1$, then $\sigma_\kappa^2 \rightarrow 0$ and the stochastic cycle reduces to the stationary deterministic cycle:

$$\psi_t = \psi_0 \cos \lambda_c t + \psi_0^* \sin \lambda_c t, \qquad t = 1, \ldots, T. \tag{2}$$

Schwing and Mendelssohn [1997] show how to put the other terms into state-space format.

[11] In all of our state-space models the different components are estimated simultaneously by maximum likelihood methods, and our oscillatory terms are stochastic and adaptive. This allows the models to deal with possible asymmetry in the data as reported by *An* [2004] and *Rodgers et al.* [2004].

[12] The STAMP software [*Koopman et al.*, 2000] was used for model estimation. The program can handle all forms of the state-space model and provides a range of diagnostic tools to analyze the fit of each model. When a time series has missing data, the state-space methodology is capable of producing estimates of the hyperparameters (these are the variance terms and AR parameter in the Kalman filter) as well as the missing data points; however, the STAMP software has not implemented this capability. Where only one or two data points were missing, such as in the Darwin SLP series, they were linearly interpolated. When many points were missing, a shorter series was used. For this reason, our analysis of the Darwin SLP series begins in 1882 while the Tahiti SLP series starts in 1933 even though both original series begin in 1882. The NOI series runs from 1950–2003. For each model, extensive checking for lack of fit was performed on the residuals and the smoothed innovations, including test of normality of the innovations [see *Harvey and Koopman*, 1992; *Koopman et al.*, 2000]. The model chosen for each series was the one that had the minimum AIC value and showed no lack of fit in the residuals.

3. Results

[13] The best state-space model for the SOI consists of a trend, a deterministic seasonal, and a 4.1 year stochastic cycle. The trend is relatively level until the mid 1950's, and then begins a consistent decline (Figure 1a, note that for comparison purposes the negative of the SOI trend is shown in this figure). The stochastic cycle clearly delineates the El Niño/La Niña events in its relative minima and maxima, in many ways more clearly than does the original series (Figure 2), since both the trend and the higher frequency variations have been filtered out.

[14] However, an examination of the component SLP series that make up the SOI, Tahiti and Darwin, shows that differencing these series in an index obscures some of the underlying dynamics. The best model for Tahiti has a constant trend, a deterministic seasonal, and two cycles (the lower frequency cycle is discussed below; the other is a

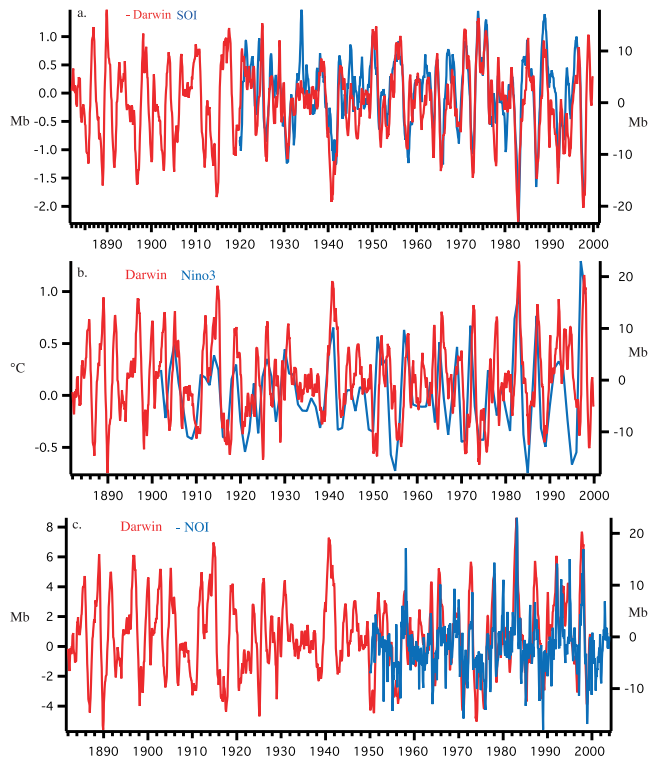

Figure 2. Comparison of the stochastic cycles from the best state-space model for (a) negative Darwin SLP (red) and the SOI (blue); (b) Darwin SLP (red) and the NINO3 temperature series (blue); (c) Darwin SLP (red) and the negative NOI (blue).

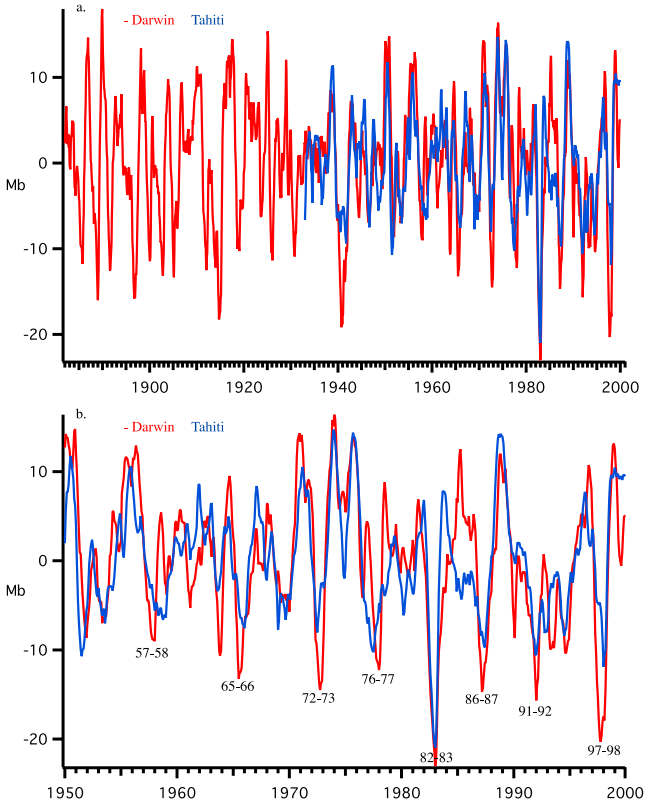

Figure 3. (a) The estimated stochastic cycle for Tahiti SLP (blue) and the negative Darwin SLP stochastic cycle (red). (b) Same as in (a) but zoomed-in for 1950–2001. The major El Niños as defined by *Schwing et al.* [2002] are labeled.

nearly deterministic high-frequency cycle), while the best model for Darwin consists of a trend, a deterministic seasonal, and a stochastic cycle with a period of 3.85 years (see Figure 1a for the trend term and Figure 3 for the cycle).

[15] The Darwin trend is almost identical to the negative of the SOI trend (Figure 1a), and the stochastic cycle term does just as well at identifying El Niño events as either the SOI or the stochastic cycle estimated from the SOI. As Tahiti has a constant trend, the long-term trend term in the SOI is due solely to changes at Darwin. The estimated Tahiti cycle and the negative of the Darwin cycle are very similar (Figure 3a). However, closer examination of the two series since 1950 (Figure 3b), shows no consistent pattern in their differences during El Niño events. For some El Niños (e.g., 1982–83), both Darwin and Tahiti contribute to the minimum in the SOI series. However for most events, the contribution of Darwin and Tahiti are not equal, and most of the cyclic behavior in the SOI is captured by the Darwin series.

[16] The best model for the yearly NINO3 series also includes a trend term and a stochastic cycle, with many of the same features of the Darwin decomposition (see Figure 1a for the trend term, Figure 2 for the cycle). Although NINO3 was estimated from yearly data and Darwin from monthly data, both the trends and the cycles are very similar (the trends have an r of 0.94 if we correlate the NINO3 trend with the June values of the Darwin trend; other months produce similar results). Both trends have inflection points around 1920–21, 1940 and 1956, with an increase in the slope in 1971 (Figure 1a).

[17] The best model for the NOI is also a trend, a deterministic seasonal, and a stochastic cycle with a period of 4.77 years (see Figure 1a for the trend term, Figure 2 for the cycle). While the sharp increase since the mid 1950's is the same as for Darwin and NINO3 (which is not surprising since the NOI is the pressure at the North Pacific High minus Darwin), there are also stronger inflection points in the NOI trend in the early 1970's, the late 1980's and the late 1990's. The cyclic terms also reflect significant differences even though Darwin SLP is part of the index (Figure 2).

[18] The damping factor ρ in the estimated stochastic cycles for the tropical Pacific series are quite high (0.94 for the SOI, 0.92 for Darwin, 0.91 for Tahiti), giving the series a longer "memory", so that two or three higher amplitude events in a short time period (e.g., the 1990's) are not inconsistent with the assumption of stationarity. The best model for the NOI has a smaller damping factor (0.68). The relative "memory" of a large event that lasts two cycles in the NOI will remain for five cycles in the tropical indices. Thus, the contribution of "shocks" to ENSO signals in the extratropics is shorter-lived than in the tropical Pacific. The NOI also displays different inflection points than the SOI, Darwin and NINO3 trends, suggesting that long-term climate variability in the Pacific may involve independent tropical and extratropical atmospheric forcing, which may stimulate the ocean at different times.

4. Discussion

[19] A series of papers have debated whether El Niños have become more frequent in recent years [*Trenberth and Hoar*, 1997; *Harrison and Larkin*, 1997; *Rajagopalan et al.*, 1997]. As Rajagopalan et al. point out, the choice of model can affect the outcome of any test for increased occurrence. *Trenberth and Hoar* [1997] assume a stationary ARMA model, while we have shown these indices are composed of a nonstationary trend and a stationary but stochastic cyclic term, and therefore are nonstationary in nature. The stationary stochastic cycles produced by the state-space models reflect the oscillation between El Niño and La Niña events and, due to their stationarity, do not support the idea that El Niños have become more frequent (a constant probability of occurrence does not imply a uniform count through time).

[20] The NINO3 trend term has been increasing, particularly since the early 1950's, so that in a model assuming a constant trend, more El Niño events (per *Trenberth and Hoar* [1997]), as defined by this index, will be seen as time progresses. A stationary stochastic cycle is the best fit to the detrended NINO3 series from the class of models we have examined, and this model shows no lack of fit to the data based on tests of the model residuals (i.e., plots of the standardized residuals, cusum and cusum-squared tests, and residuals tests for autocorrelation and significant spectral power). Thus this increasing trend in the NINO3 series since the early 1950's appears to explain the discrepancy in the debate.

[21] Moreover, if there were an asymmetry in the data, as reported by *An* [2004] and *Rodgers et al.* [2004], that was not being captured by the state-space model, this should be seen in at least one of the residual tests. No such asymmetry is seen in the residuals, either because our model compo-

nents are estimated simultaneously and the cyclic term is stochastic, or there is no asymmetry in the series.

[22] However, while the frequency of El Niño events does not appear to have changed, there is some evidence that the amplitudes of the events have increased in recent years. The state-space decomposition assumes that the amplitudes of the cycle are normally distributed. A density plot (not shown) of the smoothed estimates of the stochastic cycle of the NINO3 observations (a density plot calculates a histogram of the observations and fits a probability density estimate to the histogram) is slightly long-tailed, mainly because of a few exceptionally large values in recent years. A Q-Q plot (not shown) of the stochastic cycle (the Q-Q plot compares the quantiles of a standardized normal distribution versus the quantiles of the standardized observed data) also suggests that there are slightly more observations in the higher and lower tails than would be expected from a normal distribution, and that these observations are from the later years (large positive values in 1983, 1987, 1988, 1997; large negative values in 1984, 1985, 1995, 1996).

[23] These outlier events suggest the amplitude of the cyclic components may be increasing in recent years, but it is premature to tell. If the roughly stationary cyclic components of these series are combined with the trends (Figure 1b), we see that ENSO events are now starting from a higher level, leading to a stronger El Niño (weaker La Niña) signal in the atmosphere and ocean. For NINO3, for example, the background sea surface temperature for recent El Niño events is more than 0.5°C warmer than for events prior to 1950 (Figure 1b), meaning that recent El Niños are likely to have a stronger tropical Pacific signal, even though the stochastic ENSO cyclic component can be adequately modeled as a stationary process.

[24] Based on the estimated trends, the levels of these series in recent decades have changed by an amount equal to 30–50% of the amplitude of their corresponding annual cycle or cyclic ENSO term (Figures 1 and 3). The state-space decomposition has been a key tool in showing the independence between the ca. 4-year cyclical behavior of ENSO and what may be a global climate trend signal that has accelerated in the past 50 years, which combine to create the observed indices. While the source of the trend is not revealed by this analysis, it is clearly an important component of the climate signals of these commonly used indices.

[25] **Acknowledgments.** We thank Richard Parrish, Michael Mann and two anonymous reviewers for comments on earlier versions of this paper. This research was supported by the NOAA FATE program.

References

Akaike, H. (1973), Information theory and an extension of the maximum likelihood principle, in *Second International Symposium on Information Theory*, edited by B. N. Petrov and F. Csaki, pp. 267–281, Akademiai Kiado, Budapest.

An, S. (2004), Interdecadal changes in the El Nino-La Nina asymmetry, *Geophys. Res. Lett.*, *31*, L23210, doi:10.1029/2004GL021699.

Durbin, J., and S. J. Koopman (2001), *Time Series Analysis by State-Space Methods*, 253 pp., Oxford Univ. Press, New York.

Harrison, D. E., and N. K. Larkin (1997), Darwin sea level pressure, 1876–1996: Evidence for climate change?, *Geophys. Res. Lett.*, *24*, 1779–1782.

Harvey, A. C. (1989), *Forecasting, Structural Time Series Models, and the Kalman Filter*, 554 pp., Cambridge Univ. Press, New York.

Harvey, A. C., and S. J. Koopman (1992), Diagnostic checking of unobserved components time series models, *J. Bus. Econ. Stat.*, *10*, 377–389.

Horel, J., and J. M. Wallace (1981), Planetary-scale atmospheric phenomena associated with the Southern Oscillation, *Mon. Weather Rev.*, *109*, 813–829.

Koopman, S. J., A. C. Harvey, J. A. Doornik, and N. Shephard (2000), *STAMP 6.0: Structural Time Series Analyser, Modeler, and Predictor*, 203 pp. Timberlake Consult., London.

Mann, M. E., E. P. Gille, R. S. Bradley, M. K. Hughes, J. T. Overpeck, F. T. Keimig, and W. S. Gross (2000), Global temperature patterns in past centuries: An interactive presentation, *IGBP Pages/World Data Cent. Paleoclimatol. Data Contrib. Ser. 2000-075*, NOAA/NGDC Paleoclimatol. Program, Boulder, Colo.

Mendelssohn, R., F. B. Schwing, and S. J. Bograd (2003), Spatial structure of subsurface temperature variability in the California Current, 1950–1993, *J. Geophys. Res.*, *108*(C3), 3039, doi:10.1029/2002JC001568.

Mendelssohn, R., F. B. Schwing, and S. J. Bograd (2004), Nonstationary seasonality of upper ocean temperature in the California Current, *J. Geophys. Res.*, *109*, C10015, doi:10.1029/2004JC002330.

Philander, G. (1990), *El Niño, La Niña and the Southern Oscillation*, 293 pp., Elsevier, New York.

Rajagopalan, B., U. Lall, and M. A. Cane (1997), Anomalous ENSO occurrences: An alternate view, *J. Clim.*, *10*, 2351–2357.

Rodgers, K. B., P. Friederichs, and M. Latif (2004), Tropical Pacific decadal variability and its relation to decadal modulations of ENSO, *J. Clim.*, *17*, 3761–3774.

Schwing, F. B., and R. Mendelssohn (1997), Increased coastal upwelling in the California Current System, *J. Geophys. Res.*, *102*, 3421–3438.

Schwing, F. B., T. Murphree, and P. M. Green (2002), The Northern Oscillation Index (NOI): A new climate index for the northeast Pacific, *Prog. Oceanogr.*, *53*, 115–139.

Trenberth, K. E. (1984), Signal versus noise in the Southern Oscillation, *Mon. Weather Rev.*, *112*, 326–332.

Trenberth, K. E. (1997), On the definition of El Niño, *Bull. Am. Meteorol. Soc.*, *78*, 2771–2777.

Trenberth, K. E., and T. J. Hoar (1996), The 1990–1995 El Niño–Southern Oscillation event: Longest on record, *Geophys. Res. Lett.*, *23*, 57–60.

Trenberth, K. E., and T. J. Hoar (1997), El Niño and climate change, *Geophys. Res. Lett.*, *24*, 3057–3060.

Trenberth, K. E., and D. J. Shea (1987), On the evolution of the Southern Oscillation, *Mon. Weather Rev.*, *115*, 3078–3096.

S. J. Bograd, R. Mendelssohn, D. M. Palacios, and F. B. Schwing, Pacific Fisheries Environmental Laboratory, Southwest Fisheries Science Center, 1352 Lighthouse Avenue, Pacific Grove, CA 93950, USA. (roy.mendelssohn@noaa.gov)